ELSEVIER

Journal of Molecular Catalysis A: Chemical 141 (1999) 63–71

JOURNAL OF MOLECULAR CATALYSIS A: CHEMICAL

Translational energy of desorbing product and kinetic change at steady state in carbon monoxide oxidation on platinum(557)

Gengyu Cao [a], Yoshiyuki Seimiya [b], Tatsuo Matsushima [a,*]

[a] *Catalysis Research Center, Hokkaido University, Sapporo 060-0811, Japan*
[b] *Graduate School of Environmental Earth Science, Hokkaido University, Sapporo 060-0811, Japan*

Abstract

Velocity distributions of desorbing product CO_2 were studied in the CO oxidation on Pt(557) over a wide range of surface temperatures, in both the active and inhibited regions at the steady state. The translational energy of CO_2 in the active region, where the reaction is in a first order with respect to CO, is very high and it is insensitive to the surface temperature. It decreases sharply with increasing CO partial pressure in the boundary region. In the inhibited region, where the reaction is retarded by CO, the translational energy is relatively low and increases with increasing surface temperature.

Keywords: Desorption; Oxidation; Velocity distribution; Carbon dioxide; Platinum; Carbon monoxide; Stepped single crystal surfaces

1. Introduction

Velocity measurements of desorbing products are requisite for dynamic studies of surface reactions. An excess translational energy is found in the product CO_2 in CO oxidation on platinum metals [1,2]. Combined with internal energy measurements, the determination of this excess energy will provide the energy partition in reactive desorption events on individual sites [3–6]. This paper reports for the first time the velocity of desorbing product CO_2 in both active regions, where the reaction is in a first order with respect to CO, and inhibited regions, where the reaction is inhibited by CO, on a stepped $Pt(557) = (s)6(111) \times (001)$ surface. The translational energy of desorbing product decreased quickly near the critical CO pressures where the kinetics switched from the active region to the inhibited. This sharp kinetic change is to be expected, since it is commonly observed in CO oxidation on platinum metals [7–9].

The dependence of product velocity on surface temperature has been one of the great subjects of debate in this field, since it is believed to yield information about the energy accommodation in the desorption event [10]. Nevertheless, the relationship is not yet clear because the velocity measurements reported so far have not been performed under suitable conditions. The modulated molecular beam scattering used since the pioneering work by Becker et al. [11] can be applied when surface tempera-

* Corresponding author. Tel.: +81-11-706-3695; Fax: +81-11-706-3695; E-mail: tatmatsu@cat.hokudai.ac.jp

1381-1169/99/$ - see front matter
PII: S1381-1169(98)00250-7

tures are above about 500 K because a significant amount of CO_2 production is required at the steady state. However, below this temperature, the surface is eventually covered by CO and the reaction is mostly retarded. Furthermore, the modulation sometimes obscures reaction conditions. This is because the chopping of incoming beams may cause the oxygen and CO coverages to change throughout the conditions critical for chemical kinetics [8,9]. However, this scattering method provided characteristic measurements confirming that the surface residence time of CO is in the hundred microsecond orders for CO oxidation on Pd(111) [12] and Pt(111) [13]. The residence time of oxygen adatoms is much longer. Thus, the product desorption is likely to be merely controlled by the surface structures including reactants and surface temperature, and not by the energy state of incident molecules nor their incident angle, because the relaxation of excited surface species is completed in the picosecond order [14]. These factors make a technique combining angle-resolved thermal desorption (ARTDS) and time-of-flight (TOF) measurements appropriate for dynamic studies [15]. ARTDS–TOF is useful in a wide coverage range of reactants and at low surface temperatures [2]. However, neither tem-

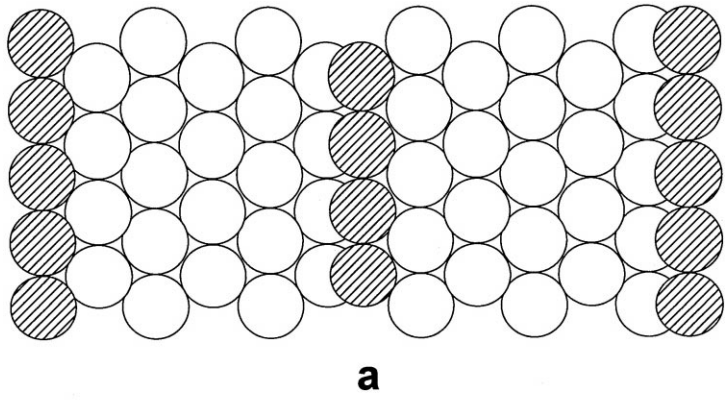

Fig. 1. (a) Surface structure of Pt(557) and (b) a (1 × 1) LEED pattern at the accelerating voltage of 80 eV.

perature dependence nor dynamics at steady state can be studied in this way because the surface temperature is scanned during measurements. Furthermore, surfaces are sometimes reconstructed during heating procedures [16].

In the present work, the velocity of product CO_2 was determined over a Pt(557) sample subjected to a constant flow of the reactant gases and fixed surface temperatures. The surface structure is shown in Fig. 1a. AR-TDS studies of this surface show CO_2 desorption dynamics similar to that exhibited by Pt(111) [17,18].

Past research on the surface temperature dependence of the velocity of desorbing product CO_2 has provided contradictory results. Poehlmann et al. first showed that the translational energy on Pt(111) could be described as $\langle E_{ex} \rangle + 2kT_s$, where $\langle E_{ex} \rangle$ is the excess energy, k is the Boltzmann constant, and T_s is the surface temperature [19]. On the other hand, Brown and Sibener once reported that the translational energy was independent of the surface temperature over Rh(111) [20]. Even so, they argued recently that the energy increased with a slope of $8.7k$ against the surface temperature [21]. Moreover, reaction conditions could not be located with certainty as being in the active or inhibited region, although the amount of adsorbed reactants changed drastically in the boundary and the velocity was sensitive to the reactant coverages [7,15,22]. The internal energy of desorbing CO_2 was determined to be higher than that expected from the surface temperature through infrared-chemi-luminescence or infrared-absorption measurements [3–6,23–26]. Mantell et al. reported increases in the asymmetric stretching temperature larger than given increases in surface temperature. They therefore predicted a simultaneous reduction in the translational energy [27]. The same group argued that the rotational energy was largely reduced with decreasing oxygen coverage [28,29]. The measurements were mostly performed at rather high pressures and high surface temperatures because of the very low sensitivity of the methodology employed. This paper is the first to report on translational energy under conditions similar to those for the infrared-work.

2. Experimental

The apparatus consisted of a reaction chamber, a chopper chamber, and an analyzer chamber. A top view of the apparatus is shown in Fig. 2. The reaction chamber had low energy electron diffraction (LEED), X-ray photoelectron spectroscopy optics, an Ar^+ gun, a mass spectrometer, and a gas-handling system that included both nozzles for free jets of CO and oxygen and variable leak-valves for backfilling the reactant gases. It was pumped by a turbo-molecular pump of 1500 l/s.

The chopper chamber was pumped with a turbo-molecular pump and a cryo-panel cooled below 40 K (with a pumping rate of about 6500 l/s). The chopper disk had slots of equal width (1 mm × 6 mm) ordered in a pseudo-random sequence (with a double sequence of 255 elements each). A time resolution of 20 μs was obtained at a rotation rate of 98.04 Hz. The trigger position was determined from curve-fitting an effusive Ar beam at room temperature to a Maxwellian distribution. The arrival time at the ionizer of the other mass spectrometer in the analyzer chamber was registered on a multichannel scaler running synchronously with the chopper blade. TOF distributions were obtained after deconvoluting the raw-TOF spectra by using a standard cross-correlation deconvolution technique [30]. The flight path between the chopper blade and the ionizer measured 377 mm, and an ion drift time of 40 μs was determined in separate experiments. The first slit was in a rectangular shape and the second was a drift tube 50 mm long and of 4 mm inside diameter.

Under the experimental conditions used, even when the total reactant pressure was 1×10^{-4} Torr, the energy transfer between the product CO_2 and the reactant molecules was negligible

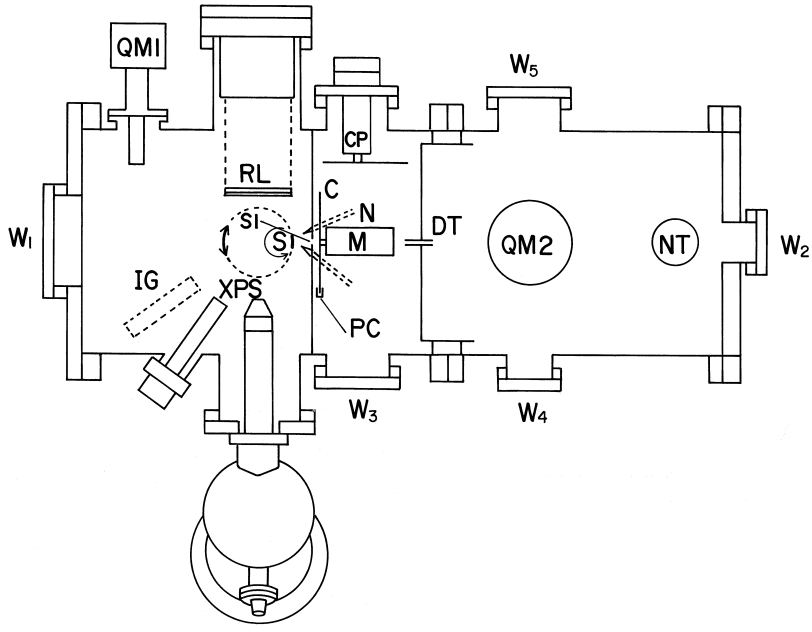

Fig. 2. Apparatus for velocity measurements at steady state. S: sample crystal, RL: reverse view LEED, S1: first slit, XPS: electron energy analyzer, IG: ion gun, QM 1 and 2: quadrupole mass spectrometer, C: random chopper, M: motor, PC: photo-cell for trigger, CP: cryogenic plate, N: gas nozzle, W1 ~ 5: window, NT: liquid nitrogen-cooled plate.

because the mean free path was about 2 m long. A platinum(557) crystal (MaTeck, Germany) was mounted on top of the manipulator and rotated to change the desorption angle (polar angle, θ). It was cleaned in the standard procedure and was annealed in vacuo up to 1150 K [22]. The LEED pattern at this stage showed a sharp (1×1) structure as shown in Fig. 1b.

3. Results

3.1. Kinetic studies

The steady-state CO_2 production rate was monitored in angle-integrated form by the mass spectrometer in the reaction chamber and in angle-resolved form by a second mass spectrometer in the analyzer chamber. No essential difference was observed in kinetics. The dependence on the surface temperature is shown in Fig. 3a. The CO_2 rate was negligible below 450 K, but it increased rapidly to a maximum with increasing surface temperature before decreasing again at higher values. The maximum was shifted to higher values with increasing total pressure, so long as CO partial pressure (P_{CO}) was close to that of oxygen (P_{O_2}). The maximum became broad at $P_{CO} < P_{O_2}$ showing a rather constant rate below 640 K.

The CO pressure dependence was characterized by sharp transitions at certain P_{CO} values. Below these values, the reaction was first-order in CO and independent of the surface temperature, whereas above them, it was of a negative-order with respect to CO and sensitive to the temperature. Hereafter, the former is named the 'active region' and the latter the 'inhibited region.' The results at 3×10^{-5} Torr O_2 are shown in Fig. 4a. The critical P_{CO} value increased with increasing O_2 pressure and also with increasing surface temperature. Such kinetics was observed in the 1×10^{-6} Torr to 1×10^{-3} Torr O_2 range.

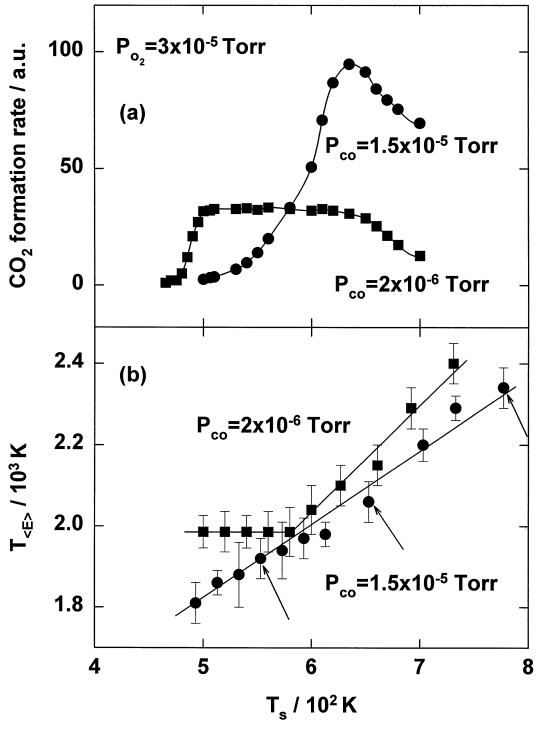

Fig. 3. (a) Variation of steady-state CO_2 formation rate with surface temperatures at different CO pressures and a fixed O_2 value. The rate was monitored in angle-integrated form. (b) Translational temperature of desorbing CO_2 under the above conditions. The arrows show the positions for velocity distributions in Fig. 6.

3.2. Velocity distribution

Angular distributions of CO_2 are slightly different in the two regions. The distribution showed a $\cos^7(\theta - 3)$ form in the active region when the angle was varied in a plane perpendicular to the step edges. The desorption is collimated 3° off the surface normal, and this is consistent with the earlier work by using AR-TDS [17]. However, it also showed a broader distribution of $\cos^4(\theta)$ in the inhibited region.

The velocity distributions of desorbing CO_2 in the normal direction at different CO pressures are shown in Fig. 5, where the surface temperature was 593 K and the O_2 pressure was 3×10^{-5} Torr. The distributions are largely shifted from a Maxwellian distribution at the surface temperature shown by the dashed lines. The translational temperature, defined as $T_{\langle E \rangle} = \langle E \rangle / 2k$, was derived from curve-fitting to a modified Maxwellian distribution form. However, the normalized speed ratio, defined as $(\langle v^2 \rangle / \langle v \rangle^2 - 1)^{1/2} / (32/9\pi - 1)^{1/2}$, where v is the velocity of the molecule, $\langle v \rangle$ is the mean velocity, and $\langle v^2 \rangle$ is the mean square velocity, was close to unity. The resultant temperature was 2020 ± 50 K at 2.0×10^{-6} Torr of CO. It decreased to 1810 ± 50 K at 1.0×10^{-5} Torr of CO and further to 1400 ± 50 K at 5.0×10^{-5} Torr of CO. These values are plotted as a function of CO pressure in Fig. 4b. In the inhibited region, the translational temperature decreased rapidly with increasing CO pressure when the fixed oxygen pressure was at 1×10^{-5} Torr. On the other hand, this sharp decrease was already apparent in the active region when the oxygen pressure was 1×10^{-4} Torr. In both regions, the translational temperature decreased

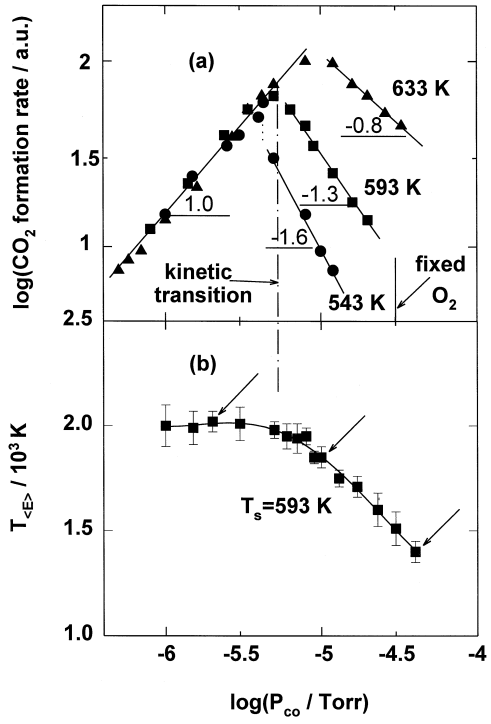

Fig. 4. Variation of CO_2 formation rate with CO pressures at different surface temperatures and a fixed O_2 pressure. The rate was monitored in angle-integrated form. The inserted numbers indicate the slope. (b) Translational temperature of desorbing CO_2 at $T_s = 593$ K. The arrows show the positions for velocity distributions in Fig. 5.

quickly with increasing desorption angle. This is consistent with an activation barrier model where a repulsive force for the desorption is exerted only along the reaction site normal.

3.3. Surface temperature dependence

The translational temperature of CO_2 is shown as a function of the surface temperature at two fixed CO pressures in Fig. 3b. The value of $T_{\langle E\rangle}$ remained around 2000 K in the active region when CO pressure was 2×10^{-6} Torr for surface temperatures of 500 K ~ 670 K. It increased with temperature at a slope of 2 above this range. It should be noticed that the CO_2 formation rate remained constant below 620 K and decreased above this temperature. On the other hand, the translational temperature increased with a slope of 1.5 in the range of 500 K ~ 800 K when the CO pressure was 1.5×10^{-5} Torr. This slope is close to the results on Pt(111) reported by Poehlmann et al. [19]. The reaction was in the inhibited region below 620 K, and the CO coverage decreased above it with increasing surface temperature. Velocity distributions at different temperatures are shown in Fig. 6. The maximum position indicated by the arrows was clearly shifted to higher values as the temperature increased. A constant translational energy in the active region and a steep increase in the inhibited region were also observed at lower O_2 pressures.

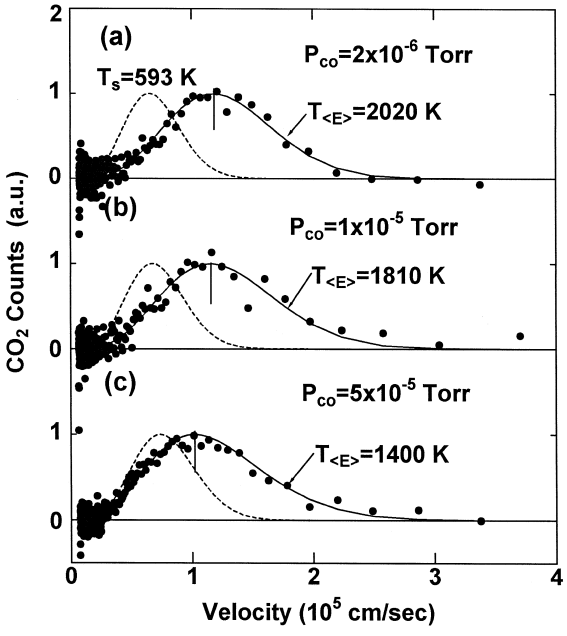

Fig. 5. Typical velocity distributions of desorbing CO_2 at $T_s = 593$ K in the (a) active, (b) transition, and (c) inhibited regions. The conditions are shown by the arrows in Fig. 4b. The solid curves were obtained by curve-fitting. Their peak positions are indicated by the vertical bars. The resultant $T_{\langle E\rangle}$ values are also inserted. A Maxwellian distribution at the surface temperature is drawn by the dashed curves.

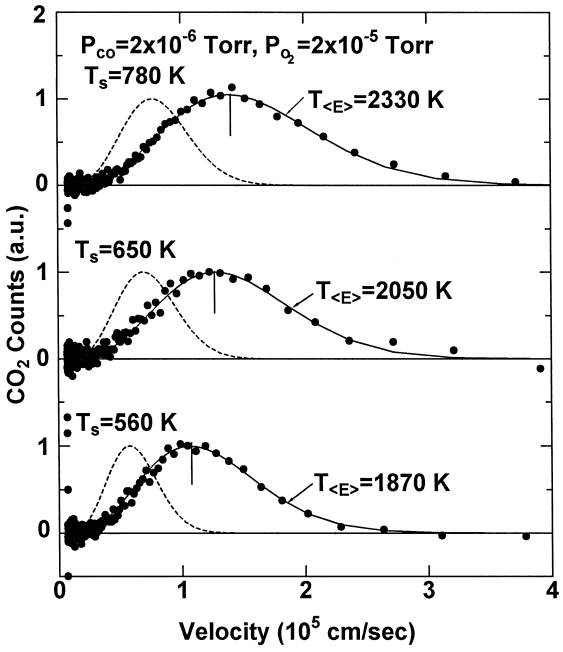

Fig. 6. Velocity distributions of desorbing CO_2 at different surface temperatures in the inhibited region at $P_{CO} = 1.5\times10^{-5}$ Torr. The conditions are shown by the arrows in Fig. 3b. The solid curves were obtained by curve-fitting. Their peak positions are shown by the vertical bars. Each $T_{\langle E\rangle}$ value is also inserted. The dashed curves show Maxwellian distributions at surface temperatures.

4. Discussion

4.1. Coverage effect

The translational energy of desorbing CO_2 showed different values in the active and inhibited regions. The observed variation cannot be explained simply by a coverage effect. It is well-known that the CO coverage increases

steeply to an equilibrium level with increasing CO pressure above the critical value, whereas oxygen adatoms are gradually suppressed as CO pressure rises to the critical value. Above this value, the adatoms decrease to negligible amounts. This change is caused by a switching of the rate-determining step from CO adsorption to oxygen dissociation under the condition that the reaction of adsorbed oxygen with adsorbed CO occurs much faster than the adsorption of either CO and oxygen [31].

The translational energy is high at high oxygen coverages, and is reduced with decreasing coverage towards the critical CO pressure. This coverage change cannot explain a further decrease of the energy above the critical CO pressure. Above the critical value, the amount of CO(a) is much higher than that of O(a), and it increases slowly with CO pressure. This CO amount is less than one-third of saturation, above which the oxygen adsorption is severely retarded. Nevertheless, the translational energy continues to decrease sharply at higher CO pressures. Furthermore, the temperature dependence in the inhibited region is quite similar to that in the active region above the bending point of approximately 600 K. The CO coverage in the inhibited region decreases with increasing temperature. However, the effect of this change does not hold above the maximum CO_2 formation temperature, because the oxygen coverage decreases and adsorbed CO is very low. The local structure of the reaction site probably plays a more important role in realizing the translational energy than the average coverage does. This phenomenon was not noticed in the ARTDS–TOF work, where both coverages were high [2].

4.2. Temperature effect

The following relation was derived for the mean kinetic energy from the simple activation barrier model [32–34],

$$\langle E\rangle = kT_s\left\{(\epsilon+1)^2+1\right\}/(\epsilon+1), \qquad (1)$$

where the parameter ϵ is defined as $\epsilon = E_b/kT_s$. E_b is the height of the activation barrier for *dissociative adsorption* of CO_2. This desorption model is over-simplified because only one-dimensional repulsive potential is considered and the variation of energy partition into the internal modes is ignored. However, it may reasonably be considered to predict characteristic behavior of the reaction sites in a qualitative sense. The value $\langle E\rangle$ remains invariant for $\epsilon \gg 1$ in surface temperature, where the kinetic energy is solely determined by the barrier height. This is consistent with observations in the active region. On the other hand, it would increase with a slope of $2k$ with the surface temperature for $\epsilon \ll 1$, where a full accommodation should be obtained. This characteristic is probably consistent with that in the inhibited region where the translational energy decreases towards the surface temperature. Thus, different reaction sites are suggested to be operative in the two regions.

The $\langle E\rangle$ value in the active region is about 2000 K, yielding $E_b = 8$ kcal/mol. This value is high enough to keep the $\langle E\rangle$ value constant below 600 K. The $\langle E\rangle$ value decreased below 1400 K in the inhibited region and the corresponding value of E_b should be less than 3 kcal/mol. However, this value is too small to predict the observed $\langle E\rangle$ value at high temperatures.

The oxidation of CO on platinum metals is likely to take place on oxygen adsorption sites because of the high mobility of CO [2,35]. On the present surface, there are six-atom-wide terraces of a (111) structure and one-atom-high steps of a (001) structure. According to the angular distribution measurements, the reaction is likely to take place mostly on the (111) terraces.

The barrier height depends on the distance of the activated state from the surface metal plane. It should decrease with increasing distance because the repulsive force between nascent CO_2 and the surface is due to a Pauli repulsion. This distance may be reduced on reaction sites surrounded by oxygen adatoms, because the oxy-

gen atoms are located deeply on the surface. In fact, oxygen on Pt(111) is 0.85 Å from the metal plane [36]. On the other hand, the activated state may be far from the metal plane when the reaction site is surrounded by CO sitting on platinum atoms. This consideration leads to the prediction that CO_2 leaves the surface with a high kinetic energy in the active region, and the product molecules are not strongly repulsed in the other. In other words, the energy transfer from activated CO_2 to the surface may take place quickly on the CO-covered surfaces. This prediction should be examined by internal energy measurements.

Mantell et al. reported that the internal energy of desorbing CO_2 over polycrystalline platinum increased more than an increase in the surface temperature and predicted a reducing translational energy at higher temperatures. This is not consistent with the present observation. Here, we have to consider another possibility that the energy partition itself depends on the surface temperature. The potential energy of the activated state of CO_2 formation on Pt(111) was estimated about 30 kcal/mol above the vacuum level at small coverages although it was shifted towards smaller values at higher coverages [13]. A large amount of the potential energy is released when CO_2 is formed. However, only about 20% of the energy is converted into the translational form. The internal modes of CO_2 receive more energy, about 25% of the potential energy, according to infrared chemi-luminescence analysis [25]. This indicates that the energy is largely (about 50%) transferred into surface modes. This transfer may be reduced at higher temperatures as predicted from smaller energy accommodation coefficients at elevated temperatures in scattering experiments of CO_2 over platinum [37].

5. Summary

The velocity distribution of desorbing product CO_2 was studied in the CO oxidation on a Pt(557) surface at steady state. The translational energy of CO_2 is very high and insensitive to the surface temperature in the active region. It decreases sharply with increasing CO partial pressure in the boundary region where the reaction switches into the region inhibited by CO. The translational energy in the latter is relatively low and increases with increasing surface temperature. Different accommodations are predicted on the reaction sites in both regions according to the simple activation barrier model.

Acknowledgements

This work was partly supported by a COE special equipment program in 1996 of the Ministry of Education, Science, Sports and Culture of Japan and also a Grand-in-Aid No. 06403012 for General Scientific Research from the Ministry.

References

[1] J.A. Barker, D.J. Auerbach, Surf. Sci. Rep. 4 (1985) 1.
[2] T. Matsushima, Heterogeneous Chemistry Review 2 (1995) 51.
[3] K. Kunimori, H. Uetsuka, T. Iwade, T. Watanabe, S. Ito, Surf. Sci. 283 (1993) 58.
[4] H. Uetsuka, K. Watanabe, K. Kunimori, Chem. Lett., 1995, 633.
[5] H. Uetsuka, K. Watanabe, K. Kunimori, Surf. Sci. 363 (1996) 73.
[6] H. Uetsuka, K. Watanabe, H. Ohnuma, K. Kunimori, Chem. Lett., 1996, 227.
[7] T. Engel, G. Ertl, Adv. Catal. 28 (1979) 1.
[8] T. Matsushima, M. Hashimoto, I. Toyoshima, J. Catal. 58 (1979) 303.
[9] M. Ehsasi, D. Frank, J.H. Block, K. Christmann, F.S. Rys, W. Hirschwald, J. Chem. Phys. 91 (1989) 4949.
[10] J.C. Tully, Annu. Rev. Phys. Chem. 31 (1980) 319.
[11] C.A. Becker, J.P. Cowin, L. Wharton, D.J. Auerbach, J. Chem. Phys. 67 (1977) 3394.
[12] T. Engel, G. Ertl, J. Chem. Phys. 69 (1978) 1267.
[13] C.T. Campbell, G. Ertl, H. Kuipers, J. Segner, J. Chem. Phys. 73 (1980) 5862.
[14] E.J. Heilweil, M.P. Cassasa, R.R. Cavanagh, J.C. Stephensen, Annu. Rev. Phys. Chem. 40 (1989) 143.
[15] T. Matsushima, K. Shobatake, Y. Ohno, K. Tabayashi, J. Chem. Phys. 97 (1992) 2783.
[16] T. Matsushima, Y. Ohno, K. Nagai, J. Chem. Phys. 94 (1991) 704.

[17] Y. Ohno, J.R. Sanchez, A. Lesar, T. Yamanaka, T. Matsushima, Surf. Sci. 382 (1997) 221.
[18] K.H. Allers, H. Pfnür, P. Feulner, D. Menzel, J. Chem. Phys. 100 (1994) 3985.
[19] E. Poehlmann, M. Schmitt, H. Hoinkes, H. Wilsch, Surf. Sci. 287–288 (1993) 269.
[20] L.S. Brown, S.J. Sibener, J. Chem. Phys. 90 (1989) 2807.
[21] J.I. Colonell, K.D. Gibson, S.J. Sibener, J. Chem. Phys. 103 (1995) 6677.
[22] Y. Ohno, T. Matsushima, H. Uetsuka, J. Chem. Phys. 101 (1994) 5319.
[23] D.A. Mantell, S.B. Ryali, B.L. Halerm, G.L. Haller, J.B. Fenn, Chem. Phys. Lett. 81 (1981) 185.
[24] L.S. Brown, S.L. Bernasek, J. Chem. Phys. 82 (1985) 2110.
[25] G.W. Coulston, G.L. Haller, J. Chem. Phys. 95 (1991) 6932.
[26] D.J. Bald, R. Kunkel, S.L. Bernasek, J. Chem. Phys. 104 (1996) 7719.
[27] D.A. Mantell, K. Kunimori, S.B. Ryali, G.L. Haller, J.B. Fenn, Surf. Sci. 172 (1986) 281.
[28] D.A. Mantell, S.B. Ryali, G.L. Haller, Chem. Phys. Lett. 102 (1983) 37.
[29] D.A. Mantell, K. Kunimori, S.B. Ryali, G.L. Haller, Am. Chem. Soc. Div. Pet. Chem. Prepr. 29 (1984) 904.
[30] G. Comsa, R. David, B.J. Schumacher, Rev. Sci. Instrum. 52 (1981) 789.
[31] T. Matsushima, D.B. Almy, J.M. White, Surf. Sci. 67 (1977) 89.
[32] W. van Willigen, Phys. Lett. A 28 (1968) 80.
[33] G. Comsa, R. David, B.J. Schumacher, Surf. Sci. 95 (1980) L210.
[34] G. Comsa, R. David, Chem. Phys. Lett. 49 (1977) 512.
[35] J.E. Reutt-Robey, D.J. Doren, Y.J. Chabal, S.B. Christman, Phys. Rev. Lett. 61 (1988) 2778.
[36] K. Mortensen, C. Klink, F. Jensen, F. Besenbacher, I. Stensgaard, Surf. Sci. 220 (1989) L701.
[37] D.A. Mantell, S.B. Ryali, G.L. Haller, J.B. Fenn, J. Chem. Phys. 78 (1983) 4250.